

# Microstructures of Developed Composite Graphite-Resin Electrodes

Isaiah Adesola Oke<sup>1</sup>, Bolaji Aremo<sup>2\*</sup>, Dayo Adeyemi Isadare<sup>2</sup>, Olusegun Emmanuel Olorunniwo<sup>2</sup>, Sodruddeen Abolore Ayodeji<sup>2</sup>, Gbemi Faith Abass<sup>3</sup>, Ayodele Abeebe Daniyan<sup>2</sup>

<sup>1</sup>Department of Civil Engineering, Obafemi Awolowo University, Ile-Ife, Nigeria

<sup>2</sup>Department of Materials Science and Engineering, Obafemi Awolowo University, Ile-Ife, Nigeria

<sup>3</sup>Department of Materials Science and Engineering, College of Mechanics and Material, Hohai University, Nanjing, China

Email: \*bolaji\_aremo@yahoo.com

**How to cite this paper:** Oke, I.A., Aremo, B., Isadare, D.A., Olorunniwo, O.E., Ayodeji, S.A., Abass, G.F. and Daniyan, A.A. (2023) Microstructures of Developed Composite Graphite-Resin Electrodes. *Materials Sciences and Applications*, 14, 526-534. <https://doi.org/10.4236/msa.2023.1412035>

**Received:** October 30, 2023

**Accepted:** December 24, 2023

**Published:** December 27, 2023

Copyright © 2023 by author(s) and Scientific Research Publishing Inc.

This work is licensed under the Creative Commons Attribution International License (CC BY 4.0).

<http://creativecommons.org/licenses/by/4.0/>



Open Access

## Abstract

This paper focuses on the effects of compaction on the microstructure of graphite-resin electrochemical treatment electrodes. This was with a view to understanding the relationships between forming parameters and some performance-limiting structural parameters of the electrode. Graphite resin electrodes were developed from graphite rods reclaimed from primary cells. The rods were crushed to powder of various particle sizes and compressed into the graphite-resin electrodes. The microstructure of the graphite electrode was observed, effects of compaction force and particles sizes distribution on the microstructure of the electrodes were observed. SEM/EDX revealed that there is a lack of homogeneity in the distribution of micro-constituents, with compositional variations differing at the various spots. However, there is a prevalence of carbon and oxygen at almost all the spots. This tends to confirm the even distribution of the elements throughout the material. The pores in the electrodes were noticed to be uniformly sized and permeate throughout the entire structure of the electrode. These pores serve to increase the surface area of these electrodes and promote the adsorption of environmental pollutants.

## Keywords

Graphite Resin Electrodes, Microstructure, Compaction Force, Particle Size

## 1. Introduction

In recent years, electrochemical treatment of water has been demonstrated to be among the major emerging technologies for potable water and wastewater purification. This technique combines a secondary treatment technique with advanced treatment concepts. This makes the treatment technique one of the in-

interesting emerging water treatment technologies [1] [2] [3] [4]. Electrochemical treatment techniques have been mainly directed toward resolving the problems originating from the release of untreated and raw industrial wastewater into water bodies and the environment [4]. This is common in both developed and underdeveloped countries alike. Some of these countries are located in tropical climates with extreme temperatures and lower concentrations of dissolved oxygen in the surface water and industrial wastewater, thus rendering impossible the utilization of biological treatment processes. Graphite-based composite electrodes have been variously described to be exceptional for electrolyzing liquids wastes and for soil remediation. Establishing a proper utilization of graphite-based composite electrodes in the production of oxidants during electrolysis of concentrated chloride, requires electrodes that will not speedily dissolve during the electrochemical treatment processes.

This work is a follow up on previous studies in the treatment process of industrial wastewaters and surface water [5] [6] [7] [8] [9]. More information on graphite ETEs, their development and stability, and factors that influence their performance can be found in literature, such as [10]-[17].

The microstructural features of the positive ETE (anodes) and negative ETEs (cathodes) greatly influences the properties of the ETEs and the electrochemical treatment processes. The effects of particle size and shapes are important, so also are the cracks in the material and the spatially confined features such as pores. The continued advancement of optimized ETE morphologies is thus an imperative task. This study is geared toward assessing the microstructure of composite graphite-resin bonded ETEs. An understanding of the structure-related performance parameters is key in the optimal deployment and confidence in this electrode class for polluted water treatment. It is believed that the reported trend will contribute substantially to the viability of electrochemical treatment of water and aid in achieving the UN sustainable development goals.

## 2. Materials and Methods

Graphite rods were removed from discarded primary cells (Type DR20 UM-1) and were crushed and milled into powder. Milled graphite powder (GP) was separated into various particle sizes. An acknowledged mass of the milled GP was mixed with resin and shaped into 25 mm diameter by 100 mm long composite ETEs. This GP-resin composite ETE was consolidated using an indigenous extruder, plunger, and a hydraulic compaction machine. The fabricated ETE electrodes are shown in **Figure 1**.

Physical characteristics such as density and electrical resistance per unit length ( $R_{ul}$ ,  $\Omega/\text{cm}$ ) of the GP-resin composite ETEs were evaluated. Influences of the distribution of GP particles sizes, compaction force and proportion of resin on the density and electrical resistance per unit length of the ETE were evaluated. In addition, the effect of the compaction force on the microstructure of the GP-resin ETEs was investigated. This was carried out with a scanning electron microscope



**Figure 1.** The produced GP-resin ETE electrodes.

(Carl Zeiss Smart Evo 10) using the high-definition backscattered electron detector (HDBSD) and the Secondary Electron (SE) detector. The HDBSD provided compositional contrast, while the SE detector establishes the topographical image of electrode surface. Energy Dispersive Spectroscopy (EDS) was done simultaneously with the SEM analysis to assess the constituent elements in the identified phases.

### 3. Results and Discussion

**Figure 2** shows the relationship between the grain size distribution, compaction force and density of the composite ETEs. The density of the composite ETE ranges between  $1.26$  and  $1.86 \text{ g}\cdot\text{cm}^{-3}$ .

It was observed that the density values of the composite ETEs are comparable to the densities of the graphite electrodes of the primary cell. These typically have densities of between  $1.58$  and  $1.72 \text{ g}\cdot\text{cm}^{-3}$ .

Also, the noticed trend indicates that the density of the composite GP-resin ETE increases with increasing compaction force. This can be attributed to the decrease in the void (pore) in the composite ETEs at higher compaction forces. Furthermore, at a constant compaction force, density tends to increase with the diminishing particle dimensions. This can be attributed to the reduction in the voids, but this time as a result of their replacement by the resin and GP particles.

The relationship between particle dimensions, compaction force and electrical resistance per unit length of the composite ETE are presented in **Figure 3**. The figure provides additional information on the associations between  $R_{ul}$  and particle dimension of the ETE. It is observed that  $R_{ul}$  increases with increasing particle dimensions and reduces with increase in applied compaction force. These two phenomena can be explained to be as a result of the increase in the amount of the resin needed to occupy the pores due to the creation of larger voids in between bigger particles.

Furthermore, increase in the surface area of the GP-resin ETE and increase in conductivity of free elections are due to high applied compaction force. **Figure 4** shows the relationship between  $R_{ul}$  and the amount of the resin utilised at a constant GP particle dimension ( $45 \mu\text{m}$ ). This value varies between  $1.35 \times 10^{-1} \Omega/\text{cm}$  and  $2.20 \times 10^{-1} \Omega/\text{cm}$  as the resin content rises between  $0.5$  and  $10 \text{ wt}\%$  at

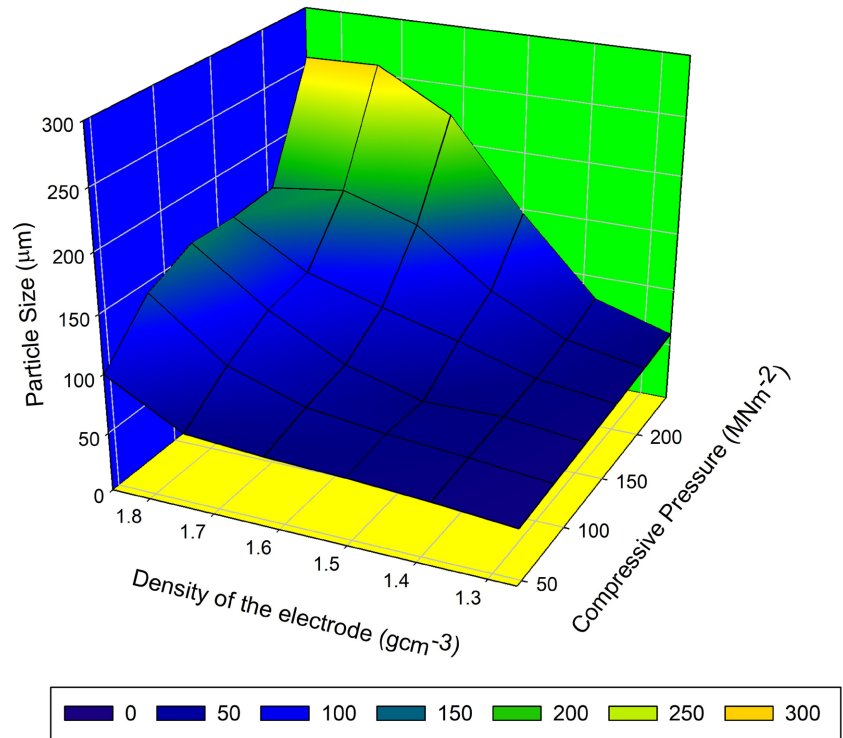


**Figure 2.** Associations between particle sizes, compaction force and density of the composite electrode at 1% resin.

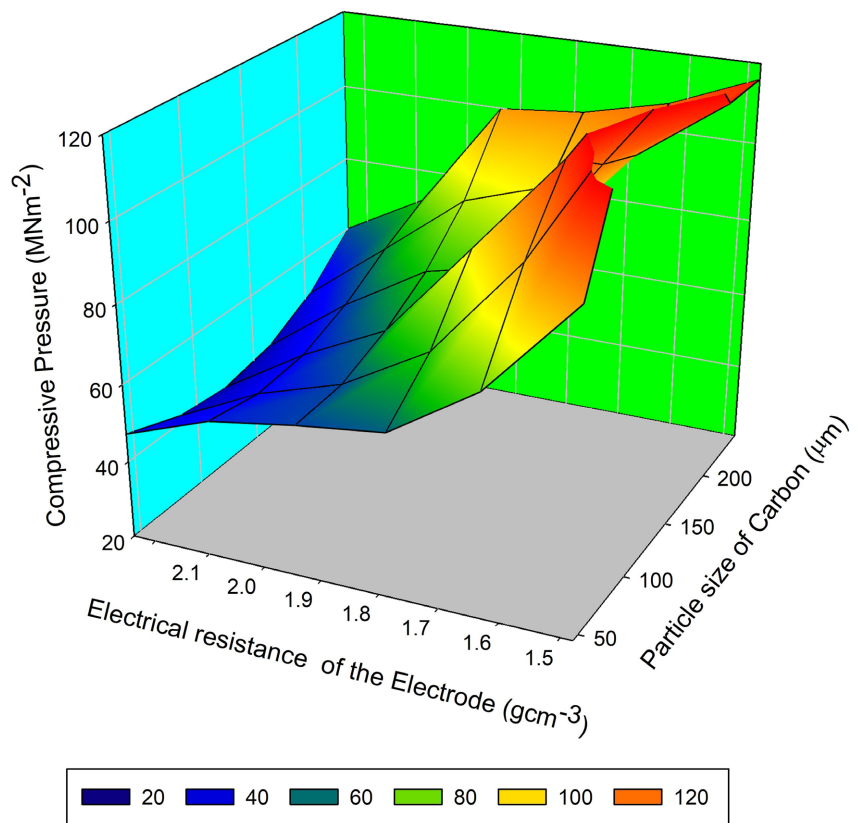


**Figure 3.** Associations between  $R_{ul}$  and particle size of graphite at 1 % resin.

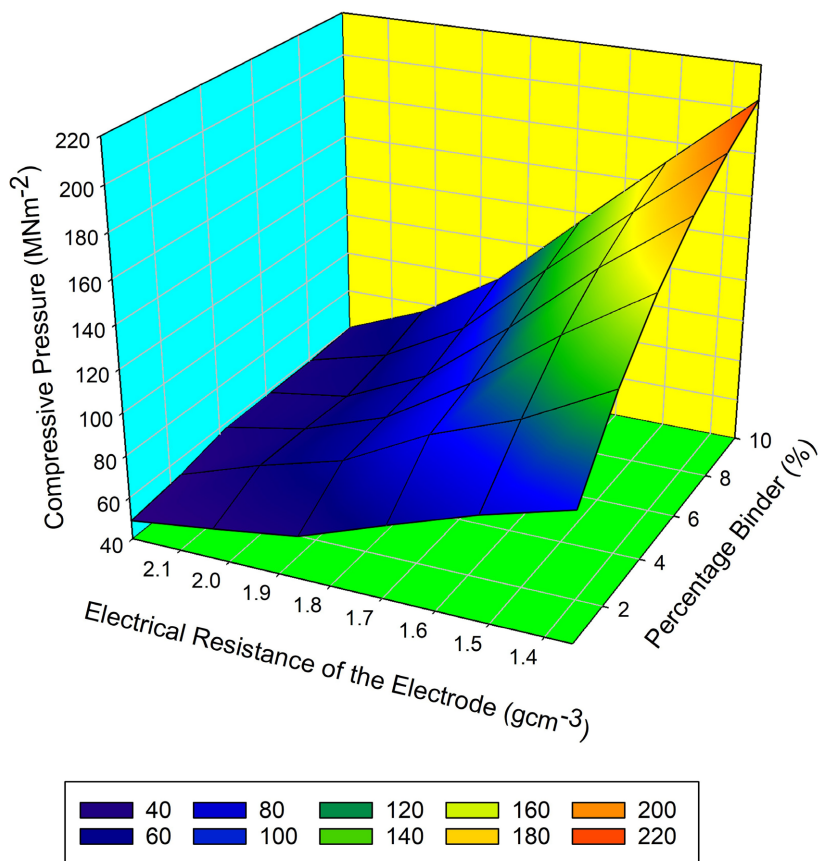


**Figure 4.** Associations between the resin and  $R_{ul}$  of the composite electrode.

compaction force ranging between 60 and 100  $\text{MN}/\text{m}^2$ . These  $R_{ul}$  were higher than typical values which are usually between  $4.5 \times 10^{-3}$  and  $1.00 \times 10^{-2} \Omega/\text{cm}$  for heat-treated graphite electrodes of the primary cell. It could thus be established from the figure that the electrical resistance of the ETE grows with a growing amount of the resin and declines with cumulative compaction force applied. The higher resin content could be said to have reduced the mean free path of the electrons and this is evidenced in the increased  $R_{ul}$  of the ETE.

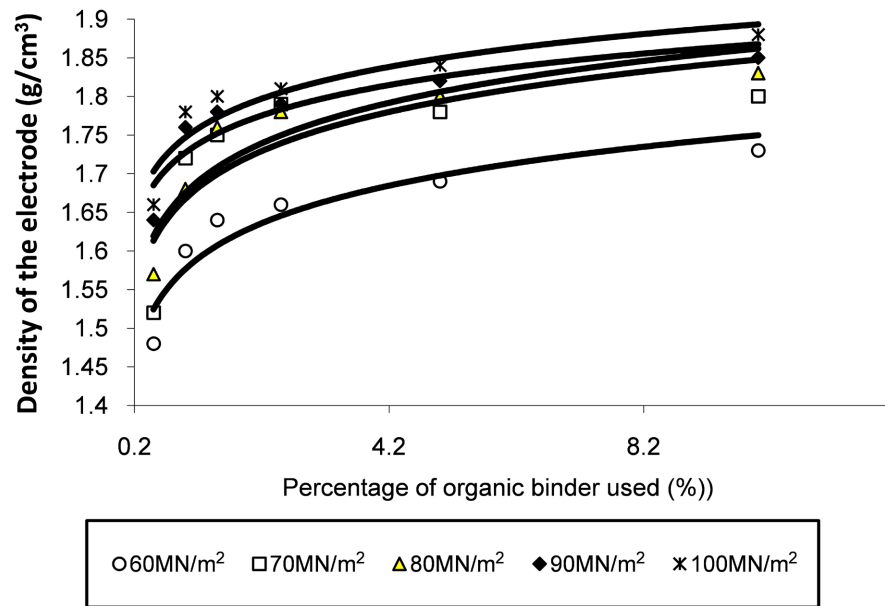
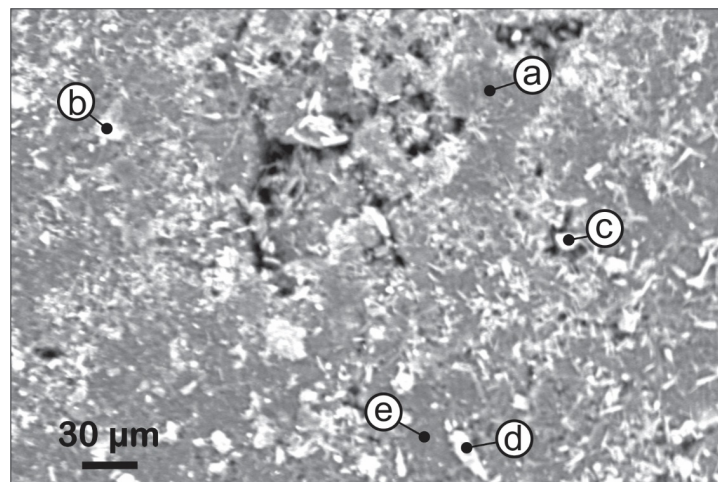
It can also be inferred that the resin, being an insulator, breaks the conductivity path through the otherwise conductive GP powder in the matrix of the ETE. **Figure 5** describes the correlation between the densities of the ETEs and the proportion of resin used. The density of the ETE rises with growing resin content and increases with increasing compaction force.

**Figure 6** presents the HDBSD image of the GP-resin ETE and the locations where spot EDS analyses were carried out. **Table 1** summarises the major elemental constituents at these locations.

The table provides a semi-quantitative view of the constituent elements and their concentration. From both the micrograph and the table, it is evident that there is inhomogeneity in the distribution of micro-constituents. There are compositional variations at the various spots, representing different types of micro-constituents. These notwithstanding however, the elements carbon and oxygen

**Table 1.** EDS compositional analysis at different locations on the ETE surface.

EDS	Elements (wt%)							
	C	Al	O	Si	Cl	Fe	Ca	Mn
Spot a	76.44	1.69	19.80	2.07	-	-	-	-
Spot b	27.49	-	8.11	-	1.02	63.38	-	-
Spot c	31.76	9.43	25.44	10.02	-	4.69	18.66	-
Spot d	25.27	-	48.57	-	-	-	25.23	0.93
Spot e	96.41	1.53	-	2.06	-	-	-	-

**Figure 5.** Associations between density of the composite ETE and percentage of resin.**Figure 6.** SEM HDBSD image of the GP-resin ETE showing locations of EDS spots.

appeared at almost all the locations. Carbon's prevalence confirms the even distribution of this element throughout the matrix. The presence of Mn and Zn can

be attributed to the fact that the graphite rods were removed from Zn - MnO primary cells. There is a likelihood that the rods have been contaminated by the chemicals of the cell's electrolyte and cathode.

**Figure 7** shows the cleaved surface of the GP-resin ETE. Numerous voids can be noticed which are uniformly distributed across the surface. These pores are important because they extend the ETE's surface area and assist in the adsorption of impurities from polluted environments. The porosity and voids results from GP powder particles stacking against each other during the forming of the ETE. Also, **Figure 8** shows a sectioned and polished cross-section of the ETE using the SE detector. The image, at 1000 $\times$  magnification presents the topological profile of the ETE microstructure. The GP particles stand out as "islands" in a background of connected groves. The groves are the pathways of sectioned connecting pores, while the "islands" are the sliced off frustrum of the GP particles. This confirms the existence of extensive cavities and interconnected pores in the ETE matrix.

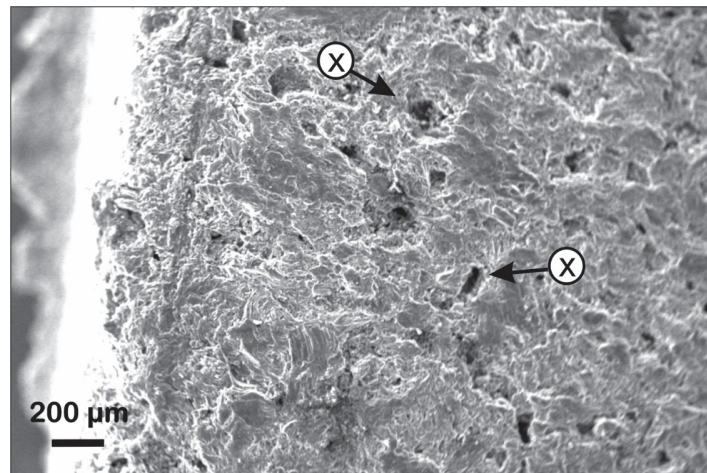


**Figure 7.** SEM of the graphite resin electrode of 75 μm particle size of graphite.

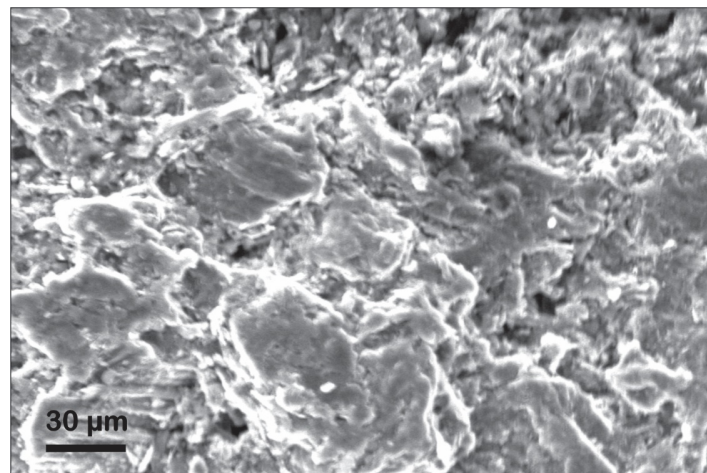


**Figure 8.** Sectioned cross-section of the GP-resin ETE showing topological surface features.

## 4. Conclusion

This work was able to underscore some structure performance parameters of the developed GP-resin ETEs. The foregoing findings showed that the ETEs produced was stable. It also showed that they possess a minimum pores distribution. These are features that make the GP-resin ETEs suitable candidates in the ECL water treatment process. Furthermore, the limit of the developed GP-resin ETEs seems to be the high internal resistance  $R_{\text{int}}$  of the electrodes. The consequence of this is that the flow of high electrical current in the ETE will cause a rise the temperature of the ETEs. However, a future application of the GP-resin ETE produced from reclaimed graphite from primary cells should be preceded with rigorous decontamination steps to rid the graphite of admixed salts from the electrolyte mix.

## Conflicts of Interest

The authors declare no conflicts of interest regarding the publication of this paper.

## References

- [1] Foti, G., Gandini, D., Comninellis, C., Perret, A. and Haenni, W. (1999) Electrochemistry of Solid-State. *Lett*, **2**, 228.
- [2] Li, Z., Qu, D. and Li, J. (2022) Effect of Different Electrofusion Processes on Microstructure of Fused Magnesia. *Refractories and Industrial Ceramics*, **62**, 541-547. <https://doi.org/10.1007/s11148-022-00639-3>
- [3] Obijole, O.A., Ogungbemi, S.T., Adekunbi, E.A., Sani, B.S., Idi, M.D. and Oke, I.A. (2022) Electrochemical Treatment of Water as an Effective and Emerging Technology. IGI Global, Hershey. <https://doi.org/10.4018/978-1-7998-7356-3.ch013>
- [4] Oke, I.A., Lukman, S., Aladesanmi, T.A., Fehintola, E.O., Amoko, S.J. and Hamed, O.O. (2020) Chapter 8 Electrochemical Treatment of Wastewater: An Emerging Technology for Emerging Pollutants. In: Shikuku, V., Ed., *Effects of Emerging Chemical Contaminants on Water Resources and Environmental Health*, IGI Global, Hershey, 133-157. <https://doi.org/10.4018/978-1-7998-1871-7.ch008>
- [5] Rangaraju, N., Raghuram, T., Krishna, V.B., Rao, K.P. and Venugopal, P. (2005) Effect of Cryo-Rolling and Annealing on Microstructure and Properties of Commercially pure Aluminium. *Materials Science and Engineering A*, **398**, 246-251. <https://doi.org/10.1016/j.msea.2005.03.026>
- [6] Oke, I.A., Umoru, L.E. and Ogedengbe, M.O. (2007) Properties and Stability of a Carbon-Resin Electrode. *Journal of Materials and Design*, **28**, 2251-2254. <https://doi.org/10.1016/j.matdes.2006.05.019>
- [7] Mahani, Y. and Zuhailawati, H. (2013). Effect of Compaction Pressure on Microstructure and Properties of Copper-Based Composite Prepared by Mechanical Alloying and Powder Metallurgy. *Advanced Materials Research*, **795**, 343-346. <https://doi.org/10.4028/www.scientific.net/AMR.795.343>
- [8] Manisankar, P., Rani, C. and Viswanathan, S. (2004) Effect of Halides in the Electrochemical Treatment of Distillery Effluent. *Chemosphere*, **57**, 961-966. <https://doi.org/10.1016/j.chemosphere.2004.07.026>
- [9] Priflinga, B., Westhoffa, D., Schmidt, D., Henning, M.H., Manke, H., Knoblauch, V.

- and Schmidt, V. (2019) Parametric Microstructure Modeling of Compressed Cathode Materials for Li-Ion Batteries. *Computational Materials Science*, **169**, Article ID: 109083. <https://doi.org/10.1016/j.commatsci.2019.109083>
- [10] Fernhndez, C., Reviejo, A.J. and Pingarrh, J.M. (1995) Development of Graphite-Poly (Tetrafluoroethylene) Composite Electrodes Voltammetric Determination of the Herbicides Thiram and Disulfiram. *Analytica Chimica Acta*, **305**, 192-199. [https://doi.org/10.1016/0003-2670\(94\)00343-K](https://doi.org/10.1016/0003-2670(94)00343-K)
- [11] Zahran, R.R (1990) Thermal Conductivity of Aluminum Reinforced Graphite Electrodes. *Materials Letters*, **10**, 93-98. [https://doi.org/10.1016/0167-577X\(90\)90038-N](https://doi.org/10.1016/0167-577X(90)90038-N)
- [12] Shigeo, S. (2012) Weibull Distribution Function Application to Static Strength and Fatigue Life of Materials. *Tribology Transactions*, **55**, 267-277. <https://doi.org/10.1080/10402004.2011.651770>
- [13] Xia, G, Huijiao, W., Juhong, Z., Xiaomeng, Y., Xiaocui, W., Gang, Y., et al. (2020) Evaluation of the Stability of Polyacrylonitrile-Based Carbon Fiber Electrode for Hydrogen Peroxide Production and Phenol Mineralization during Electroperoxone Process. *Chemical Engineering Journal*, **396**, Article ID: 125291. <https://doi.org/10.1016/j.cej.2020.125291>
- [14] Kolyagin, G.A., Kornienko, V.L., Kuznetsov, B.N. and Chesnokov, N.V. (2005) Electrical Conductivity of Hydrophobized Electrodes Fabricated from Thermally Expanded Graphite and Their Activity in Electroreduction of Oxygen. *Russian Journal of Applied Chemistry*, **78**, 1625-1630. <https://doi.org/10.1007/s11167-005-0574-7>
- [15] Wang, Z., Yang, H., Liu, Y., Bai, Y., Chen, G., Li, Y., Wang, X., Xu, H., Wu, C., and Lu, J. (2020) Analysis of the Stable Interphase Responsible for the Excellent Electrochemical Performance of Graphite Electrodes in Sodium-Ion Batteries. *Small*, **16**, Article ID: 2003268. <https://doi.org/10.1002/sml.202003268>
- [16] Geneste, F., Moinet, C., Ababou-Girard, S. and Sola, F. (2005) Stability of  $[\text{Ru}^{\text{II}}(\text{tpy})(\text{bpy})(\text{OH}_2)]^{2+}$ -Modified Graphite Electrodes during Indirect Electrolyses. *Inorganic Chemistry*, **44**, 4366-4371. <https://doi.org/10.1021/ic048231k>
- [17] Barbero, E., Fernández-Saéz, J. and Navarro, C. (2000). Statistical Analysis of the Mechanical Properties of Composite Materials. *Composites: Part B*, **31**, 375-381. [https://doi.org/10.1016/S1359-8368\(00\)00027-5](https://doi.org/10.1016/S1359-8368(00)00027-5)